Transactions, SMiRT-24
BEXCO, Busan, Korea - August 20-25, 2017
Division I (include assigned division number from I to X)

A CAVITY GROWTH MODEL INVOLVING THE SHAPE EVOLUTION OF GRAIN BOUNDARY VOIDS DURING CREEP

Jing-Dong Hu[1], Fu-Zhen Xuan[2], and Chang-Jun Liu[3]

[1] Ph.D. student, Key Laboratory of Pressure System and Safety, East China University of Science and Technology, Shanghai, China
[2] Professor, Key Laboratory of Pressure System and Safety, East China University of Science and Technology, Shanghai, China (fzxuan@ecust.edu.cn)
[3] Professor, Key Laboratory of Pressure System and Safety, East China University of Science and Technology, Shanghai, China

ABSTRACT

Referring to the Cocks and Ashby model, an improved creep deformation and lifetime prediction model was proposed. The improvement was achievement through involving the void shape changes a the grain boundary during the creep deformation. In addition, a new multiaxial ductility factor for multiaxial creep analysis has been developed based on the newly proposed model. The newly proposed model has been verified by using the experimental data and comparisons with the existing models.

INTRODUCTION

Polycrystalline metals, especially face centred cubic (*fcc)* metals like austenite steel, are commonly used in many kinds of components operating at elevated temperature. After a long-term service even at a lower stress level condition, creep induced intergranular fracture is likely to happen in these components. The primary mechanism of the onset of this fracture process is generally considered as the micro voids nucleate, grow and finally coalesce on the grain boundary. (Giessen, et al. 1995) Based on this microscope mechanism, the cavity growth models are the ‘local approach’ and try to use an isolate void growth procedure to represent the whole material’s failure process. One of the cavity growth models proposed by Cocks and Ashby (1980) describes a spherical void growth in the grain boundary slab and deduces the analytic formulas for calculating creep failure time and strain by power-law creep in an axisymmetric stress state.

However, some of the assumptions made by Cocks and Ashby (1980) are not conform to experimental observations, which may cause error. The *in-situ* observations of voids growth and coalescence in a plastic-deformed matrix conducted by Weck, et al. (2008), Hosokawa et al. (2012) and Nemcko and Wilkinson (2016) indicate that the void shape changes severely during the plastic deformation process. In fact, Cocks and Ashby themselves have already realized problem that at low triaxiality the void shape cannot be a spherical, as shown in Fig. 1(a). To solve this problem, an empirical expression α has been introduced in their paper. On the other hand, the void shape can be affected by diffusion if the void growth is controlled by diffusion. When the grain boundary diffusion rate is lower than the surface diffusion rate, the vacancies will be stacked in the voids’ ends, and accumulate into voids, which will make the spherical void shape oblate, as shown in Fig. 1(b). According to the diffusion theory, in equilibrium state, dihedral angle Ψ between tangent at voids’ end and boundary is related to the ratio of surface diffusion energy to grain boundary diffusion energy. In most of metals and alloys, this angle value is around 70º, according to Needleman and Rice (1980). Therefore, it suffices to say that the growth process of intergraunlar voids under creep deformation will lead to void shape changes.

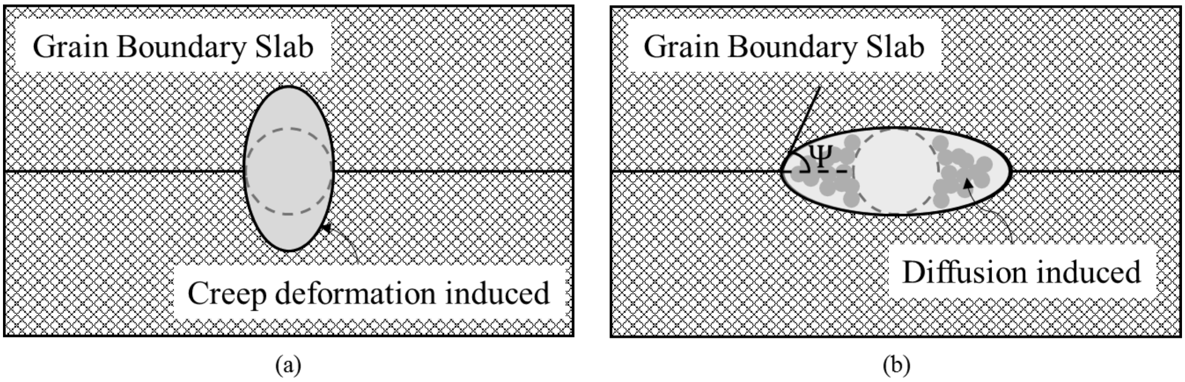

Figure 1. Some possible reasons caused void shape change, (a) creep deformation induced (b) diffusion vacancies.

The aim of this paper is to bring the void shape evolution effect into Cocks and Ashby (1980) model. Instead of using Finite Element Method (FEM), some mathematic approaches have been used to make sure that the proposed model can directly give analytical solution for creep lifetime and deformation. The assumptions and the derivation process are shown in the following chapters. The verification of this new model and applications for multiaxial creep are also shown in this paper.

MODELLING DESCRIPTION

The new model is largely based on the Cocks and Ashby model, as shown in Fig.2 left. It is assumed that all the voids in the material are nucleated at the same time t_n, and the value of t_n is often set to 0. When voids growth reaches a critical value, it is assumed that the voids coalescence and the failure of materials occur together at this time point t_f ,and this time t_f is defined as creep lifetime. The following further assumption (a)(b)(c) are the same with Cocks and Ashby :

(a) The average steady-state creep rate, when no voids are present, is:

$$\dot{\varepsilon}_{ss} = \dot{\varepsilon}_0 \left(\sigma_{eq}/\sigma_0\right)^n \tag{1}$$

Where $\dot{\varepsilon}_{ss}$ is the steady-state creep rate, σ_{eq} is the von Mises equivalent stress, $\dot{\varepsilon}_0$, σ_0 , n are the material parameters used in this power-law creep constitutive.

(b) Grain boundaries slide, so that the increase in volume of the slab containing the voids, shown in Fig. 2, is taken up by a relative rigid-body displacement of the grains on either side.

(c) The slab as a whole, being wide in comparison with its thickness, is constrained by the surrounding material to contract laterally only as the sample itself does (in simple tension it contracts at a rate $\dot{\varepsilon}_{ss}/2$).

The different assumption is here. It is assumed that the void at the initial time t_n is a sphere, but continuously evolves and becomes an ellipsoid at the failure time t_f . We consider that, at the early stage, the void volume is small so its growth is controlled by diffusion mainly. The grain boundary diffusion rate is fast enough so it is likely to see a spherical void in the nucleation stage. However, when the void gains some volume, the controlled mechanism will transform to creep deformation, which will severely change the void shape. In order to count the shape factor, a void shape factor β has been defined as the ratio of the diameter of the void projection on the grain boundary to the length of the void in the axial. β is related to the creep deformation factors, diffusion factors and creep time. In this case, only creep deformation-controlled void growth is considered. We assume β is a function of triaxiality and creep time, $\beta = f_s\left(T_r, t\right)$. The void shape factor at nucleation is 1 (i.e. spherical). The void shape factor at failure is β_c . A complete void shape evolution process is shown in Fig 2 right.

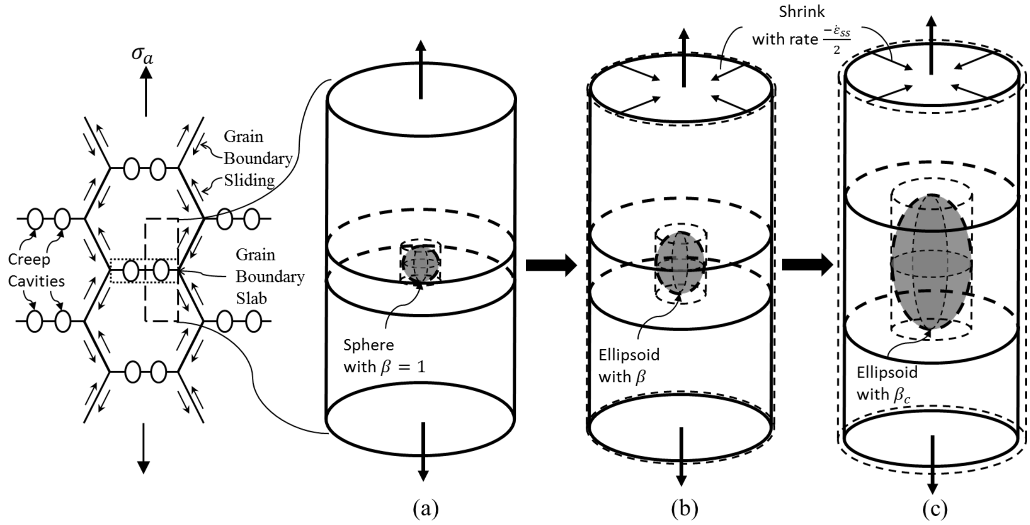

Figure 2. Evolution of the void shape, (a) void nucleation ($t = t_n$), (b) during growth ($t_n < t < t_f$), (c) void radius reach the critical value of coalescence ($t = t_f$).

In the end, this proposed model, the same as Cocks and Ashby model, is only for power-law creep. And it is only for the situation where cavity (or void) growth controlled by deformation only, or by constrained diffusion. Therefore, the void shape factor has a potential limit that it is equal or greater than 1.

VOID GROWTH UNDER UNIAXIAL TENSION

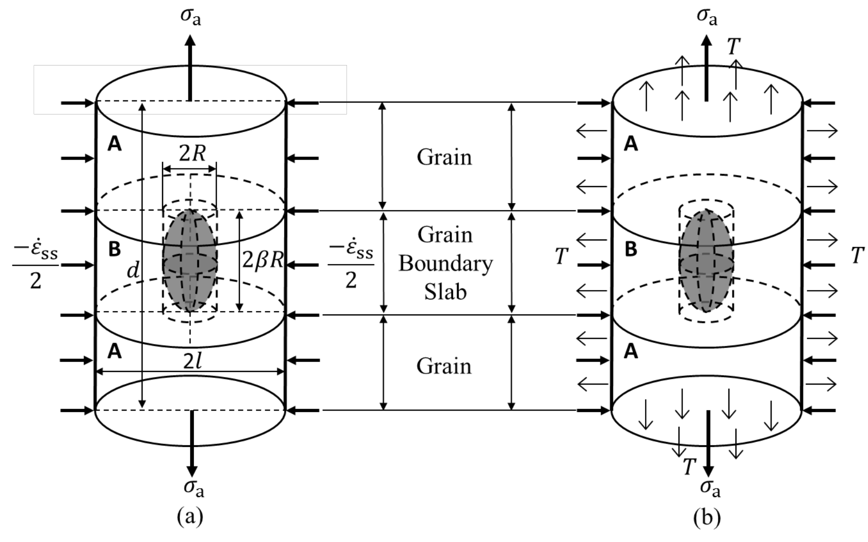

Figure 3. Void growth under remote stress (a) uniaxial stress state (b) multiaxial stress state.

The model contains a cylinder of the material centred on the void (Fig. 3) with an outer diameter equal to $2l$, the separation of voids in the boundary plane, and a height equal to the grain size d . It is assumed that the tractions on the surface of this cylinder are equal to those applied to the specimen as a whole. For the purposes of choosing a stress field (but not in the subsequent geometry), the shape of the void has been idealized as a cylinder of radius R and height $2\beta R$. Void is contained in a thick annular ring called 'Grain Boundary Slab' (region B, Fig 3). The grain boundary slab is sandwiched between two solid cylinders called 'Grain' (regions A). Then the area fraction of voids in the boundary plane at any time is:

$$f_\mathrm{h} = \left(R/l\right)^2 \tag{2}$$

Differentiating Eq.(2) with the respect of time t gives:

$$\frac{2}{R}\frac{\mathrm{d}R}{\mathrm{dt}} = \frac{1}{f_\mathrm{h}}\frac{\mathrm{d}f_\mathrm{h}}{\mathrm{dt}} - \dot{\varepsilon}_\mathrm{ss} \tag{3}$$

We assume that the stress field in the same region is equal everywhere. This simplified stress field has been proven to be an upper bound of the true stress field (Edward and Ashby (1979)). In the uniaxial tension condition, as shown in Fig. 3(a), the stress field in region A:

$$\begin{cases} \sigma_\mathrm{z} = \sigma_\mathrm{a} \\ \sigma_\mathrm{r} = \sigma_\theta = 0 \end{cases} \tag{4}$$

Where σ_a is tensile stress. σ_r, σ_θ, σ_z are the three principle stress in cylindrical coordinate.

In region B, the stress field:

$$\begin{cases} \sigma_\mathrm{z} \le \dfrac{\sigma_\mathrm{a}}{1-f_\mathrm{h}} \\ \sigma_\mathrm{r} = \sigma_\theta = 0 \end{cases} \tag{5}$$

Eq.(4) and Eq.(5) can be used to calculate strain rate in each region. According to the geometry, the whole cylinder strain rate $\dot{\varepsilon}_\mathrm{a}$ can be given:

$$\dot{\varepsilon}_\mathrm{a} \le \dot{\varepsilon}_\mathrm{ss}\left\{1 + \frac{2\beta R}{d}\left[\frac{1}{\left(1-f_\mathrm{h}\right)^\mathrm{n}} - 1\right]\right\} \tag{6}$$

And the volume change in the cylinder is:

$$\frac{1}{V}\frac{\mathrm{d}V}{\mathrm{dt}} = \dot{\varepsilon}_\mathrm{a} - \dot{\varepsilon}_\mathrm{ss} \tag{7}$$

Where V represents the volume of cylinder. According to assumption (b), the volume change of cylinder is all contributed by the void volume increase.

$$\frac{1}{V}\frac{\mathrm{d}V}{\mathrm{dt}} = \frac{1}{V}\frac{\mathrm{d}v}{\mathrm{dt}} = \frac{4}{3}\frac{R^3}{l^2 d}\frac{\mathrm{d}\beta}{\mathrm{dt}} + \frac{4\beta R^2}{l^2 d}\frac{\mathrm{d}R}{\mathrm{dt}} \tag{8}$$

Where v represents the volume of void. Combining Eq.(6), Eq.(7) and Eq.(8) gives:

$$\frac{1}{\dot{\varepsilon}_\mathrm{ss}}\frac{\mathrm{d}f_\mathrm{h}}{\mathrm{dt}} \le \frac{1}{\left(1-f_\mathrm{h}\right)^\mathrm{n}} - \left(1 - f_\mathrm{h} + \frac{2f_\mathrm{h}}{3\beta\dot{\varepsilon}_\mathrm{ss}}\frac{\mathrm{d}\beta}{\mathrm{dt}}\right) \tag{9}$$

By integrating Eq.(9), the failure time $\mathrm{t_f}$ can be given. Integration limits are:

$$\begin{cases} f_\mathrm{h} = f_\mathrm{i}, \beta = 1 \quad \text{at} \quad \mathrm{t} = \mathrm{t_n} \\ f_\mathrm{h} = f_\mathrm{c}, \beta = \beta_\mathrm{c} \quad \text{at} \quad \mathrm{t} = \mathrm{t_f} \end{cases} \tag{10}$$

Where f_i is the void area fraction at nucleation, and f_c is the void area fraction at failure, also called critical failure value. Substituting limits (10) into Eq.(9) gives the creep lifetime predication:

$$\mathrm{t_f} \ge \mathrm{t_n} + \frac{1}{\dot{\varepsilon}_\mathrm{ss}}\left[\int_{f_\mathrm{i}}^{f_\mathrm{c}} \frac{\left(1-f_\mathrm{h}\right)^\mathrm{n}}{1-\left(1-f_\mathrm{h}\right)^{\mathrm{n}+1}}\mathrm{d}f_\mathrm{h} + \int_1^{\beta_\mathrm{c}} \frac{2f_\mathrm{h}}{3\beta}\frac{\left(1-f_\mathrm{h}\right)^\mathrm{n}}{1-\left(1-f_\mathrm{h}\right)^{\mathrm{n}+1}}\mathrm{d}\beta\right] \tag{11}$$

Here the critical failure value f_c is set to 0.25 empirically. Because the relationship between β and f_h is unknown, we have to use some mathematical approaches. Let $f_\mathrm{h} = f_\mathrm{c}$ in the integral containing $\mathrm{d}\beta$, so as to reduce it:

$$\mathrm{t_f} \ge \mathrm{t_n} + \frac{1}{\left(\mathrm{n}+1\right)\dot{\varepsilon}_\mathrm{ss}}\ln\left[\frac{1}{\left(\mathrm{n}+1\right)f_\mathrm{i}}\right] + \frac{2f_\mathrm{c}}{3\dot{\varepsilon}_\mathrm{ss}}\frac{\left(1-f_\mathrm{c}\right)^\mathrm{n}}{1-\left(1-f_\mathrm{c}\right)^{\mathrm{n}+1}}\ln\beta_\mathrm{c} \tag{12}$$

Let β_c equal to 1, then Eq.(12) degrades into the same result as Cocks and Ashby model gives:

$$\mathrm{t_f} = \mathrm{t_n} + \frac{1}{(\mathrm{n}+1)\dot{\varepsilon}_{\mathrm{ss}}} \ln\left[\frac{1}{(\mathrm{n}+1) f_{\mathrm{i}}}\right] \tag{13}$$

The simultaneous system of Eq.(3), Eq.(6), Eq.(9) gives:

$$\dot{\varepsilon}_{\mathrm{a}} \le \dot{\varepsilon}_{\mathrm{ss}} + \frac{4\beta R^2}{l^2 d}\frac{\mathrm{d}R}{\mathrm{dt}} + \frac{4R f_{\mathrm{h}}}{3d}\frac{\mathrm{d}\beta}{\mathrm{dt}} \tag{14}$$

Integrating Eq.(14) between the limits (10) can give the creep failure strain, also called creep deformation. Because of the unknown relationship of R, f_{h} to β, here again, some mathematical approaches are used. We let β in the integral containing dR equal to β_c so as to enlarge it, and let $f_{\mathrm{h}} = f_{\mathrm{c}}$ and $R = \sqrt{f_{\mathrm{c}}}\, l$ in the integral containing dβ as the same reason. Then integrate Eq.(14) gives the creep deformation prediction:

$$\varepsilon_{\mathrm{f}} \le \dot{\varepsilon}_{\mathrm{ss}}\mathrm{t_f} + \frac{4\beta_{\mathrm{c}} l}{3d}\left(\sqrt{f_{\mathrm{c}}^3} - \sqrt{f_{\mathrm{i}}^3}\right) + \frac{4l}{3d}(\beta_{\mathrm{c}} - 1)\sqrt{f_{\mathrm{c}}^3} \tag{15}$$

Setting $\beta_{\mathrm{c}} = 1$, $f_{\mathrm{i}} = 0$, $f_{\mathrm{c}} = 0.25$, Eq.(15) reduces to the results almost same as Cocks and Ashby model gives:

$$\varepsilon_{\mathrm{f}} \le \dot{\varepsilon}_{\mathrm{ss}}\mathrm{t_f} + \frac{l}{6d} \approx \dot{\varepsilon}_{\mathrm{ss}}\mathrm{t_f} + \frac{0.2l}{d} \tag{16}$$

VOID GROWTH UNDER UNIAXIAL TENSION

Superimpose a hydrostatic tension T to the uniaxial tensile condition in the section 3, as shown in Fig.4 (b), and create a symmetric multiaxial stress state. We assume that the cylinder shares the same equivalent stress and triaxiality with the specimen as a whole. So the hydrostatic tension T:

$$T = 3\sigma_{\mathrm{eq}}(1 - T_{\mathrm{r}}) \tag{17}$$

Where T_{r} is the triaxiality, $T_{\mathrm{r}} = \sigma_{\mathrm{m}}/\sigma_{\mathrm{eq}}$. σ_{m} is the mean stress, $\sigma_{\mathrm{m}} = (\sigma_{\mathrm{z}} + \sigma_{\mathrm{r}} + \sigma_{\theta})/3$. Similarly, here we give the stress field in each region. The stress field in region A is:

$$\begin{cases} \sigma_{\mathrm{z}} = \sigma_{\mathrm{a}} + T \\ \sigma_{\mathrm{r}} = \sigma_{\theta} = T \end{cases} \tag{18}$$

The stress field in region B is derived by integrating the equilibrium equation:

$$\frac{\mathrm{d}\sigma_{\mathrm{r}}}{\mathrm{d}r} = \frac{\sigma_{\theta} - \sigma_{\mathrm{r}}}{r} = \frac{\mathrm{const}}{r} \tag{19}$$

Where r is the distance of a point to the void centre. Then the stress field in region B is given as:

$$\begin{cases} \sigma_{\mathrm{z}} \le \dfrac{\sigma_{\mathrm{a}}}{1 - f_{\mathrm{h}}} + T\left(\dfrac{1 + 2\ln r/R}{\ln 1/f_{\mathrm{h}}}\right) \\ \sigma_{\mathrm{r}} = T\left(\dfrac{2\ln r/R}{\ln 1/f_{\mathrm{h}}}\right) \\ \sigma_{\theta} = T\left(\dfrac{2 + 2\ln r/R}{\ln 1/f_{\mathrm{h}}}\right) \\ \text{where } l \ge r \ge R \end{cases} \tag{20}$$

Similarly, we can get equations like Eq.(6) and Eq.(9) in section 3:

$$\dot{\varepsilon}_{\mathrm{a}} \le \dot{\varepsilon}_{\mathrm{ss}}\left(1 - \frac{2\beta R}{d}\right) + \frac{2\beta R}{d}\left[\frac{\dot{\varepsilon}_{\mathrm{ss}}}{(1 - f_{\mathrm{h}})^{\mathrm{n}}}\right](1 + D)^{\mathrm{n}/2} \tag{21}$$

$$\frac{1}{\dot{\varepsilon}_{\mathrm{ss}}}\frac{\mathrm{d}f_{\mathrm{h}}}{\mathrm{dt}} \le \frac{(1+D)^{\mathrm{n}/2}}{(1-f_{\mathrm{h}})^{\mathrm{n}}} - \left(1-f_{\mathrm{h}} + \frac{2f_{\mathrm{h}}}{3\beta\dot{\varepsilon}_{\mathrm{ss}}}\frac{\mathrm{d}\beta}{\mathrm{dt}}\right) \tag{22}$$

Where D is:

$$D = 3\left[\frac{(1-f_{\mathrm{h}})}{\ln f_{\mathrm{h}}}\cdot\frac{T}{\sigma_{\mathrm{a}}}\right]^2 = 3\left[\frac{(1-f_{\mathrm{h}})(T_{\mathrm{r}}-1/3)}{\ln f_{\mathrm{h}}}\right]^2 \tag{23}$$

Now the time to failure, or the creep lifetime in multiaxial stress state is obtained by integrating Eq.(22) between the limits (10):

$$\mathrm{t_f} \ge \mathrm{t_n} + \frac{1}{\dot{\varepsilon}_{\mathrm{ss}}}\left[\int_{f_{\mathrm{i}}}^{f_{\mathrm{c}}}\frac{(1-f_{\mathrm{h}})^{\mathrm{n}}}{(1+D)^{\mathrm{n}/2}-(1-f_{\mathrm{h}})^{\mathrm{n+1}}}\mathrm{d}f_{\mathrm{h}} + \int_{1}^{\beta_{\mathrm{c}}}\frac{2f_{\mathrm{h}}}{3\beta}\frac{(1-f_{\mathrm{h}})^{\mathrm{n}}}{(1+D)^{\mathrm{n}/2}-(1-f_{\mathrm{h}})^{\mathrm{n+1}}}\mathrm{d}\beta\right] \tag{24}$$

Some mathematical approaches are used in order to successfully calculate the creep lifetime. Here we set f_{h} in the integral containing $\mathrm{d}\beta$ equal to f_{c} so as to reduce it. We get:

$$\mathrm{t_f} \ge \mathrm{t_n} + \frac{1}{\dot{\varepsilon}_{\mathrm{ss}}}\left[\int_{f_{\mathrm{i}}}^{f_{\mathrm{c}}}\frac{(1-f_{\mathrm{h}})^{\mathrm{n}}}{(1+D)^{\mathrm{n}/2}-(1-f_{\mathrm{h}})^{\mathrm{n+1}}}\mathrm{d}f_{\mathrm{h}} + \frac{2f_{\mathrm{c}}}{3}\frac{(1-f_{\mathrm{c}})^{\mathrm{n}}}{(1+D')^{\mathrm{n}/2}-(1-f_{\mathrm{c}})^{\mathrm{n+1}}}\ln\beta_{\mathrm{c}}\right] \tag{25}$$

Where D' is:

$$D' = 3\left[\frac{(1-f_{\mathrm{c}})(T_{\mathrm{r}}-1/3)}{\ln f_{\mathrm{c}}}\right]^2 \tag{26}$$

From Eq.(21) and Eq.(22), we can get expression to calculate the creep deformation under multiaxial stress state. The expression is the same as Eq.(15) but t_{f} here is from Eq.(25).

CREEP LIFETIME AND MONKMAN-GRANT RELATIONSHIP

Creep lifetime largely depends on the minimum creep rate (also called the steady-state creep rate). The famous Monkman and Grant (1956) relationship (M-G relationship) was obtained from a large amount of uniaxial creep rupture experiments and this relationship are commonly found in austenite steel. The M-G relationship is that the product of steady-state creep rate $\dot{\varepsilon}_{\mathrm{ss}}$ and creep lifetime $\mathrm{t_f}$ is a constant $\mathrm{C_{MG}}$, which is independent with temperature and uniaxial tensile stress:

$$\dot{\varepsilon}_{\mathrm{ss}}\mathrm{t_f} = \mathrm{C_{MG}} \tag{27}$$

From Eq.(12), we can know that the proposed model, and Cocks and Ashby model both obey the M-G relationship in uniaxial situation.

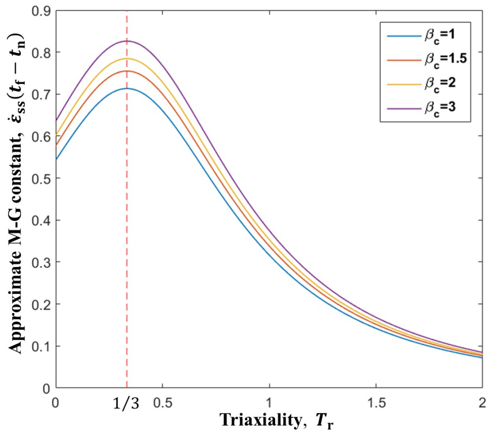

Figure 4. The relationship between triaxiality and approximate M-G constant with different void shape factor. The material parameter n and f_{i} are fixed in 3 and 0.01, respectively.

Nevertheless, in multiaxial stress state, the model predicts M-G constnt changes with triaxiality changing. Let us set n equal to 3 and f_i equal to 0.01. Since the nucleation time can be ignored, the production here is an approximate M-G constant. With different void shape factor β_c, the relationship between triaxiality and approximate M-G constant is shown as Fig. 4. From Fig. 4 we can observe that all the curves have a common axis of symmetry $T_r = 1/3$. That is because Eq.(23) is squared. Two totally different stress states, $T_r < 1/3$ and $T_r > 1/3$, are considered to be the same in this model. $T_r = 1/3$ means the uniaxial stress state and it is the maximum value point of the curve. It is suitable in $T_r = 1/3$ (i.e. pure tensile stress state). Since creep failure strain in $T_r < 1/3$ is found to be larger (Wen, et al. 2016) than that in $T_r = 1/3$, the model obviously do not provide the appropriate value in this part. So here, an announcement can be made that **the proposed model is only suitable for the pure tensile stress state** (i.e. $T_r > 1/3$). Another observation from Fig. 4 is that the void shape factor has a positive effect on static creep strain. It means that the voids which is more like a lens tends to have a better ductility than the voids which have a crack-like shape.

Since the void shape factor β_c is also related with triaxiality, here, we mark the β_c in uniaxial stress state as $\beta_{c,u}$, and in multiaxial β_{c,T_r}. In practice, only $\beta_{c,u}$ can be conveniently obtained by uniaxial creep experimental data. Since β_c represents the void shape at failure, we know that when $T_r \to \infty, \beta_{c,T_r} \to 1$ (i.e. when triaxiality approaches to infinity (i.e. a hydrostatic stress field in the case), the void will tend to be a sphere). And when $T_r \to 1/3, \beta_{c,T_r} \to \beta_{c,u}$. According to this presumption, here we artificially introduced a formula to calculate β_{c,T_r}:

$$\beta_{c,T_r} = \left(\beta_{c,u} - 1\right)\exp\left(\frac{1}{3} - T_r\right) + 1 \tag{28}$$

The multiaxial creep rupture test is hard to conduct. Most recently, Kobayashi et al. (2017) have published some biaxial and triaxial tensile creep rupture data. Those data have been analysed by us and transformed to what we want, and used to fit with our model. The triaxial and biaxial fitting result are shown in Fig. 5(a) and Fig. 5(b). From Fig. 5 we can see the proposed model gives a good match with the experimental data.

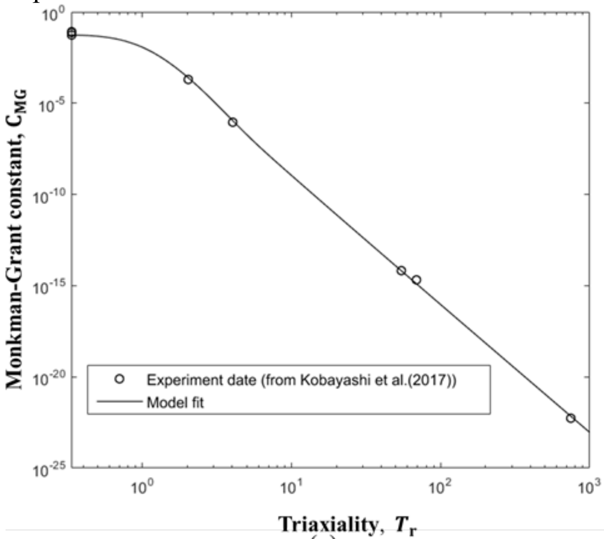

(a)

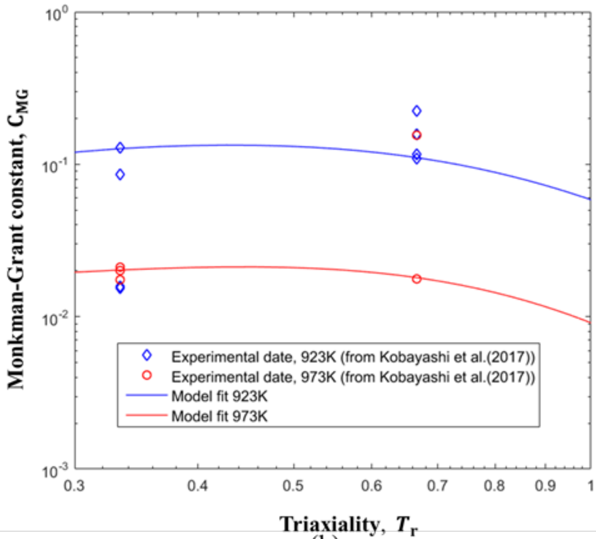

(b)

Figure 5. The relationship between M-G constant and triaxiality: (a) Triaxial test in 973K, (b) Biaxial test in 973K (red) and 923K (blue). Data are transformed from Kobayashi et al. (2017).

MULTIAXIAL DUCTILITY FACTOR

Creep strain is one of the important parameters in strength design in elevated temperature. In engineering practice, structures often under the complex multiaxial stress state. Calculating creep strain in multiaxial stress state can be realized by multiaxial creep constitutive formulas. However, to determine the material parameters in those formulas need to fit with the material creep data in a required multiaxial stress state. The quantity of multiaxial stress state is infinite, so it is impossible to get all the data through experiments. Therefore, in practice engineers often use conversion formulae to get the required multiaxial strain data based on uniaxial creep experimental data. Cocks and Ashby model gives a conversion formula, but it is proven to be not so accurate and need to be modified comparing with the experimental data provided by Wichtmann (2002). Then, Spindler (2004) defines the *multiaxial ductility factor* (MDF) as the ration of multiaxial creep deformation to uniaxial creep deformation in the same equivalent von Mises stress. Spinder's formula for calculating multiaxial ductility factor considers both creep deformation and diffusion controlled void growth mechanism and adopted by British R5 standards. Spindler(2014) later renames MDF to cavity growth factor, but definition almost keeps unchanged. Later, basing on the work of Cocks and Ashby (1980), Yatomi et al. (2014), and Wen and Tu (2014) proposed their own multiaxial ductility factor. However, their modifications are empirical. In this chapter, we provide multiaxial ductility factor by the proposed model, which is not only based on Cocks and Ashby model but also improves its physical core.

MDF is represents as:

$$\varepsilon_{\mathrm{f}} = \mathrm{MDF} \cdot \varepsilon_{\mathrm{f,u}} \tag{29}$$

Where ε_{f} is the creep deformation in multiaxial stress state and $\varepsilon_{\mathrm{f,u}}$ is the uniaxial creep deformation. From Eq.(12), Eq.(15) and Eq.(25), we can obtain MDF:

$$\begin{aligned} \mathrm{MDF} = &\left\{ \mathrm{t_n}\dot{\varepsilon}_{\mathrm{ss}} + \frac{1}{\mathrm{n}+1}\ln\left[\frac{1}{(\mathrm{n}+1)f_{\mathrm{i}}}\right] + \frac{2f_{\mathrm{c}}}{3}\frac{(1-f_{\mathrm{c}})^{\mathrm{n}}}{1-(1-f_{\mathrm{c}})^{\mathrm{n}+1}}\ln\beta_{\mathrm{c,u}} + \mathrm{f}(\beta_{\mathrm{c,u}}) \right\} \\ &\Bigg/ \left\{ \mathrm{t_n}\dot{\varepsilon}_{\mathrm{ss}} + \int_{f_{\mathrm{i}}}^{f_{\mathrm{c}}} \frac{(1-f_{\mathrm{h}})^{\mathrm{n}}}{(1+D)^{\mathrm{n}/2}-(1-f_{\mathrm{h}})^{\mathrm{n}+1}}\mathrm{d}f_{\mathrm{h}} + \frac{2f_{\mathrm{c}}}{3}\frac{(1-f_{\mathrm{c}})^{\mathrm{n}}}{(1+D')^{\mathrm{n}/2}-(1-f_{\mathrm{c}})^{\mathrm{n}+1}}\ln\beta_{\mathrm{c},T_{\mathrm{r}}} + \mathrm{f}(\beta_{\mathrm{c},T_{\mathrm{r}}}) \right\} \end{aligned} \tag{30}$$

D is from Eq.(23) and D' is from Eq.(24). Where the function $\mathrm{f}(\beta_{\mathrm{c}})$ is:

$$\mathrm{f}(\beta_{\mathrm{c}}) = \frac{4\beta_{\mathrm{c}} l}{3d}\left(\sqrt{f_{\mathrm{c}}^3} - \sqrt{f_{\mathrm{i}}^3}\right) + \frac{4l}{3d}(\beta_{\mathrm{c}}-1)\sqrt{f_{\mathrm{c}}^3} \tag{31}$$

With the help of Eq.(28), now we can use the proposed model to calculate MDF curve with all parameters obtained in uniaxial. Fig. 6 shows the comparison between proposed model and models from Cocks and Ashby (1980), Rice and Tracy (1969), Manjoine (1975, 1982), Wen and Tu (2014). Some experimental data from Wichtmann and Spindler have together involved in the comparison. In Fig. 6, three families of curves, which is decorated with shadow lines, are calculated by proposed model and Eq. (37) with $\beta_{\mathrm{c,u}} \in [1,3]$. Where red family of curves is the proposed model with $l/d = 0.1$, $f_{\mathrm{i}} = 0.01$; blue with $l/d = 0.05$, $f_{\mathrm{i}} = 0.0001$; green with $l/d = 0.5$, $f_{\mathrm{i}} = 0.000001$. Rather than changing with the only material parameter n like other models, the proposed model changes with three more material parameters: l/d represents as average void number in grain boundary, f_{i} represents as the area fraction of a void at nucleation and $\beta_{\mathrm{c,u}}$ represents as the void shape factor at failure under uniaxial stress state. All the parameters used in the proposed model have specific physical meanings. With the help of these parameters, MDF curves calculated by this proposed new model exhibit their flexibility to fit with almost all the experimental data with different type of austenite steels.

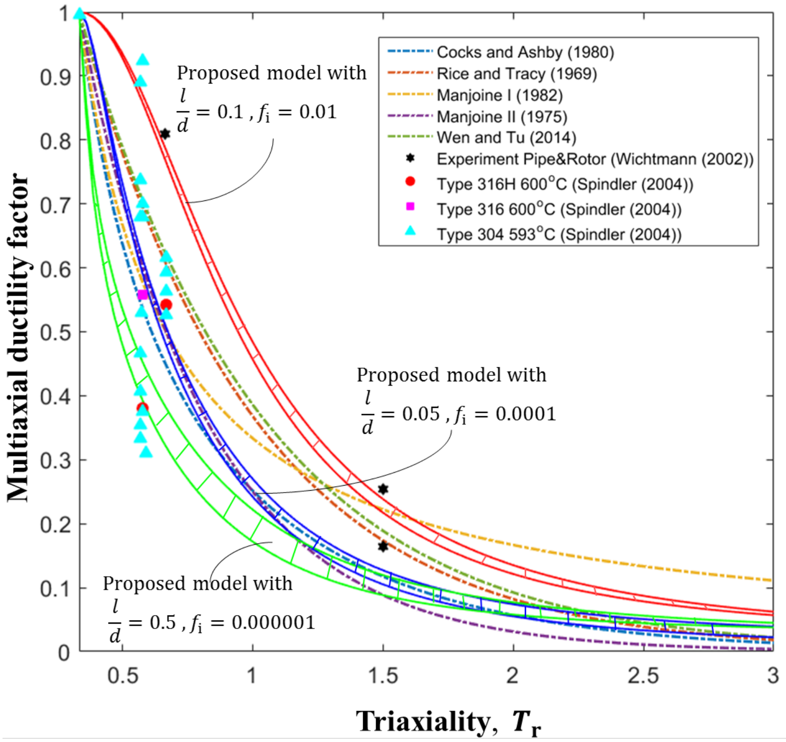

Figure 6. Multiaxial ductility factor calculated from different models with $n = 3$. The experimental data of pipe and rotor are from Wichtmann (2002), the rest data are from Spindler (2004).

CONCLUSIONS

Due to the widely usage of austenite steel in nuclear industry, it is of impendency to improve the accuracy of typical forecasting models, and simultaneously keep its ease of operation in engineering. Based on the Cocks and Ashby model, the newly proposed model adds the void shape evolution effect, and thus has an excellent ability in predicting the creep lifetime and deformation of different types of austenite steel.

Under uniaxial stress state, the proposed model obeys the Monkman and Grant (M-G) relationship. However, the model predicts that in multiaxial stress state, the M-G relationship breaks. The nonlinear relationship between M-G constants and triaxiality given by the proposed model is checked by the biaxial and triaxial tensile creep experimental data provided by Kobayashi et al. (2017).

For applications, the proposed model can give analytic solution for calculating Multiaxial Ductility Factor (MDF), which serves as a scale factor to convert uniaxial creep deformation into multiaxial creep deformation. With the help of four meaningful parameters, MDF curves calculated by the proposed model has a better flexibility than other existing models, and catches most experimental data.

It is worth noting that the proposed model is developed under the situation of triaxiality $T_r \geq 1/3$ (i.e. pure tensile stress state) because of Eq.(23) being squared. The totally different stress state $T_r < 1/3$ and $T_r > 1/3$ are considered to be the same in this model. In addition, the proposed model uses von Mises stress, which cannot deflect the difference between the compressive stress and the tensile stress. From physical aspect, the proposed model is largely based on Cocks and Ashby model, which only considers creep deformation, or constrained diffusion controlled void growth.

ACKNOWLEDGEMENT

This work is funded by the National Natural Science Foundation of China (Grant Nos. 51325504 and 51475167). All authors greatly thank for the support of NSFC.

REFERENCES

Giessen, E. V. D., Burg, M. W. D. V. D., Needleman, A., Tvergaard, V. (1995). "Void growth due to creep and grain boundary diffusion at high triaxialities," *Journal of the Mechanics and Physics of Solids*, Elsevier, US, 43 123-165.

Cocks, A. C. F., Ashby, M. F. (1980). "intergranular fracture during power-law creep under multiaxial stresses," *Metal Science*, 14 395-402.

Weck, A., Wilkinson, D.S., Maire, E., Toda, H. (2008). "Visualization by X-ray tomography of void growth and coalescence leading to fracture in model materials," *Acta Materialia*, Elsevier, US, 56 2919-2928.

Hosokawa, A., Wilkinson, D. S., Kang, J., Maire, E. (2012). "Effect of triaxiality on void growth and coalescence in model materials investigated by X-ray tomography," *Acta Materialia*, Elsevier, US, 60 2829-2839.

Nemcko, M. J., Wilkinson, D. S. (2016). "On the damage and fracture of commercially pure magnesium using x-ray microtomography," *Materials Science and Engineering: A*, Elsevier, CH, 676 146-155.

Needleman, A., Rice, J.R. (1980). "Plastic creep flow effects in the diffusive cavitation of grain boundaries," *Acta Metallurgica*, 28 1315-1332.

Edward, G. H., Ashby, M. F. (1979) "Intergranular fracture during power-law creep," *Acta Metallurgica*, 27 1505-1518.

Monkman, F. C., Grant, N. J. (1956) "An empirical relationship between rupture life and minimum creep rate in creep-rupture tests," *In proc. ASTM* 56 593-620.

Kobayashi, H., Ohki, R., Itoh, T., Sakane, M. (2017). "Multiaxial creep damage and lifetime evaluation under biaxial and triaxial stresses for type 304 stainless steel," *Engineering Fracture Mechanics*, Elsevier, ENG.

Wichtmann, A. (2002) "Evaluation of Creep Damage due to Void Growth under Triaxial Stress States in the Design of Steam Turbine Components," *JSME International Journal. Series A*, 45 72-76.

Spindler, M. W. (2004). "The multiaxial creep ductility of austenitic stainless steels," *Fatigue and Fracture of Engineering Materials and Structures*, 27 273-281.

Rice, J. R., Tracey, D. M. (1969). "On the ductile enlargement of voids in triaxial stress fields," *Journal of the Mechanics and Physics of Solids,* Elsevier, US, 17 201-217.

Hull, D., Rimmer, D. E. (1959). "The growth of grain-boundary voids under stress," *Philosophical Magazine*, 4 673-687.

M.W. Spindler, (2014). "The multiaxial and uniaxial creep ductility of Type 304 steel as a function of stress and strain rate," *Materials at High Temperatures*, Taylor & Francis, ENG, 21 47-54.

Yatomi, M., Nikbin, K.M. (2014). "Numerical prediction of creep crack growth in different geometries using simplified multiaxial void growth model," *Materials at High Temperatures*, Taylor & Francis, ENG, 31 141-147.

Wen, J. F., Tu, S. T. (2014). "A multiaxial creep-damage model for creep crack growth considering cavity growth and microcrack interaction," *Engineering Fracture Mechanics*, Elsevier, ENG, 123 197-210.

Manjoine, M. J. (1982). "Creep-Rupture Behavior of Weldments," *Welding J*, 61 50-58.

Manjoine, M. J. (1975). "Ductility indices at elevated temperature," *Journal of Engineering Materials and Technology*, ASME, US, 97 156-161.